Bright nonlocal quadratic solitons induced by boundary confinement

Yizhou Zheng, Yan Gao, Jing Wang, Fang Lv, Daquan Lu,* and Wei Hu†

Guangdong Provincial Key Laboratory of Nanophotonic Functional Materials and Devices, South China Normal University, Guangzhou 510631, China

(Received 17 March 2016; published 4 January 2017)

Under the Dirichlet boundary conditions, a family of bright quadratic solitons exists in the regime where the second harmonic can be regarded as the refractive index of the fundamental wave with an oscillatory nonlocal response. By simplifying the governing equations into the Snyder-Mitchell mode, the approximate analytical solutions are obtained. Taking them as the initial guess and using a numerical code, we found two branches of bright solitons, of which the beam width increases (branch I) and decreases (branch II) with the increase of the sample size, respectively. If the nonlocality is fixed and the sample size is varied, the soliton width varies piecewise and approximately periodically. In each period, solitons only exist in a small range of sample size. Single-hump fundamental wave solitons with the same beam width in narrower samples can be, if the second harmonics are connected smoothly, jointed to be a multihump soliton in a wider sample whose size is the sum of those for the narrower ones. The dynamical simulation shows that the found solitons are unstable.

DOI: 10.1103/PhysRevA.95.013808

I. INTRODUCTION

Quadratic solitons, which were theoretically predicted in the 1970s [1,2] and first observed in the 1990s [3,4], have attracted extensive interest and been widely investigated in past decades (Refs. [5–8] and references therein). Because of the fast and strong electronic nonlinearity in $\chi^{(2)}$ media, quadratic solitons have potential applications such as in ultrafast all-optical switching [9]. The beam-trapping mechanism of the quadratic solitons crucially differs from its counterpart in Kerr-type media. In Kerr-type media the solitons come into being because of the balance between the diffraction and/or dispersion and the self-focusing, which is caused by the beam-induced distribution of the nonlinear refractive index. However, in quadratic media, the self-trapping of solitons comes from the rapid exchange of energy and phase between two or more optical fields during quadratic optical parametric process. The phase mismatch value is an important parameter for the quadratic solitons. The conventional technique on controlling the phase mismatch value (e.g., to make the interacting fields phase matched or nearly phase matched) is realized based on birefringence and temperature tuning. Compared to the conventional technique, the technique of quasi-phase matching (QPM) makes a great step forward. The QPM technique is as such: the nonlinear susceptibility is artificially modulated periodically; therefore an additional phase mismatch is induced. The additional mismatch can compensate the inherent mismatch partly or entirely. Based on the QPM technique, it is possible to take advantage of the highest coefficients of the second-order nonlinear susceptibility tensor. Therefore QPM is a promising technique for the reduction of the power level for the beam trapping and large phase shift in quadratic media. The problem of solitons [10,11] in QPM quadratic media and related issues, such as the modulation instability [12] and the optical switch [13,14], have been investigated in detail.

The characteristics of quadratic solitons are determined by some key parameters in the coupling equations. Considering coupling between the fundamental wave (FW, E_1) and its second harmonic (SH, E_2) in a type I phase-matching case, the coupling equations are

$$i\frac{\partial E_1}{\partial z} + d_1\frac{\partial^2 E_1}{\partial x^2} + E_1^* E_2 e^{-i\beta z} = 0, \tag{1}$$

$$i\frac{\partial E_2}{\partial z} + d_2\frac{\partial^2 E_2}{\partial x^2} + E_1^2 e^{i\beta z} = 0, \tag{2}$$

where the term $\partial_x^2 E_{1,2}/\partial x^2$ represents beam diffraction or pulse dispersion and β is the phase mismatch. Readers can refer to previous references, such as Refs. [15,16], for the detailed derivation of Eqs. (1) and (2). Assuming the soliton solution in the forms $E_1(x,z) = a_1\phi_1(x)e^{i\lambda z}$ and $E_2(x,z) = a_2\phi_2(x)e^{i2\lambda z + i\beta z}$, and using the scaling parameters $a_1^2 = \lambda^2|(d_2/2d_1)|$, $a_2 = \lambda$, $\tau = x|\lambda/d_1|^{\frac{1}{2}}$, $s_j = \mathrm{sgn}(\lambda d_j)$, and $\alpha = (2+\beta/\lambda)|d_1/d_2| > 0$, Eqs. (1) and (2) become [17]

$$s_1\frac{\partial^2\phi_1}{\partial\tau^2} - \phi_1 + \phi_1\phi_2 = 0, \tag{3}$$

$$s_2\frac{\partial^2\phi_2}{\partial\tau^2} - \alpha\phi_2 + \frac{1}{2}\phi_1^2 = 0. \tag{4}$$

Under the cascading case (i.e., $\alpha \gg 1$) $\phi_2 \simeq \phi_1^2/(2\alpha)$ and Eqs. (3) and (4) reduce to the model $s_1(\partial^2/\partial\tau^2)\phi_1 - \phi_1 + [\phi_1^2/(2\alpha)]\phi_1 = 0$, which is equivalent to the equation governing the solitons in locally responded Kerr-type media [18]. However, this local model is not valid in cases where the limit $\alpha \gg 1$ is not satisfied. In 2003 [17], Nikolov *et al.* pointed out that in general cases the model should be $s_1(\partial^2/\partial\tau^2)\phi_1 - \phi_1 + [1/(2\alpha)\int_{-\infty}^{\infty} R(\tau-\xi)\phi_1^2(\xi)d\xi]\phi_1 = 0$, which is equivalent to that for the solitons in the nonlocal Kerr nonlinear media (readers can refer to Ref. [19] for a review of nonlocal solitons). In fact, except for the soliton problem, problems such as pulse compression [20,21], localized X waves [22], and modulation instability [23] in $\chi^{(2)}$ media can also be approximately described by the nonlocal model.

*ludq@scnu.edu.cn
†huwei@scnu.edu.cn

Equations (3) and (4) can be used both in the temporal domain and the spatial domain. In the temporal domain, the readers may have the question of whether the response function is reasonable (because it seems that the effect may precede the cause). In fact, in the derivation of Eqs. (3) and (4) from Eqs. (1) and (2), we take an important assumption that the fields E_1 and E_2 are steady-state (soliton) solutions. Thus, the response function is actually describing the relation between the fundamental wave and its second harmonic (the relation must be satisfied when the FW and SH are soliton solutions), rather than describing the dynamic influence of the FW on its refractive index which in turn affects its evolution [24]. Therefore, for the soliton problem in the temporal domain, the model Eqs. (3) and (4) are reasonable and are not in violation of the law of causality.

The parameters s_1 and s_2 play key roles in determining the soliton type and its stability. The previous works show that in the case $s_2 = +1$ the response function is an exponentially decay one [i.e., $R(\tau) = (\sqrt{\alpha}/2)\exp(-\sqrt{\alpha}|\tau|)$]; and in this case the stable bright (dark) solitons exist if $s_1 = +1$ ($s_1 = -1$) [17,25]. In the case $s_2 = -1$ the response function becomes an oscillatory one [i.e., $R(\tau) = (\sqrt{\alpha}/2)\sin(\sqrt{\alpha}|\tau|)$]; there exist bright (dark) solitons if $s_2 = +1$ [25,26] ($s_2 = -1$ [25]), but the solitons are all unstable under the no-boundary conditions (the no-boundary conditions mean that the FW and its SH propagate in infinite media; and the propagation is therefore not influenced by boundary confinement). In 2014, our research shows that, under the Dirichlet boundary conditions, there can exist stable bright solitons in the case $s_2 = -s_1 = -1$ [27].

In this paper we go one step further to investigate the bright solitons in the regime $s_2 = s_1 = -1$ under the Dirichlet boundary conditions. The parameter combination $s_2 = s_1 = -1$ can be realized in the spatial domain: the parameters s_1 and s_2 in Eqs. (3) and (4) are jointly determined by d_1, d_2, and λ, i.e., $s_{1,2} = \mathrm{sgn}(\lambda d_{1,2})$. Therefore, for a homogeneous structure in which the diffraction parameters are $d_1 \approx 2d_2 > 0$, we can get $s_{1,2} = -1$, provided that $\lambda = -|\lambda|$. In the following it is shown that in the case $s_2 = s_1 = -1$, there can exist bright solitons under the Dirichlet boundary conditions (under the no-boundary conditions only dark solitons are found in this combination of s_1 and s_2 in previous works).

The rest of this paper is organized as follows. In Sec. II, we make an approximation on the model Eqs. (3) and (4) and simplify them into the Snyder-Mitchell mode (SMM [28]) under the Dirichlet boundary conditions. Based on the SMM we get the approximate analytical solutions of the bright solitons in the case $s_1 = s_2 = -1$. In Sec. III, taking the analytical solutions as the initial trial solutions, we get the numerical solutions of the bright solitons of the precise model Eqs. (3) and (4). It is found that there exist two branches of bright solitons and the characteristics of the two branches are discussed. We conclude in Sec. IV.

II. SIMPLIFIED MODEL AND THE ANALYTICAL SOLITON SOLUTION

Because of the mathematical complication, it is difficult to get the precise analytical solutions of Eqs. (3) and (4). To get the analytical solutions, here we make an approximation on Eqs. (3) and (4) and simplify them into the SMM. Based on the SMM, we get the approximate analytical soliton solutions, which are taken as the initial trial solutions to get the numerical precise soliton solutions in Sec. III.

For Eqs. (3) and (4), ϕ_2 can be regarded as the nonlinear refractive index induced by ϕ_1; therefore it is possible for the FW to become a soliton if the SH "seen"by the FW is concave or convex. When $s_2 = +1$ ($s_2 = -1$), the response function is an exponentially decaying one (oscillatory one) and the SH soliton is bell-like (oscillatory). For both cases, suppose that (i) the FW is narrow enough so that the part of the SH "seen" by the FW is concave or convex (as is shown in the following figures) and (ii) the SH and FW are all symmetric about the sample center $x = 0$, then we can make a Taylor expansion on the SH ϕ_2 about $x = 0$:

$$\phi_2(\tau) = \phi_2(0) + \tau\phi_2'(0) + \frac{\tau^2}{2}\phi_2''(0) + \cdots . \tag{5}$$

Because the SH ϕ_2 is symmetric about $x = 0$, we can omitting the odd derivative in Eq. (5). Then truncating the remained even derivative to the order of τ^2 we get

$$\phi_2(\tau) = \phi_2(0) + \frac{\tau^2}{2}\phi_2''(0). \tag{6}$$

Therefore, in the case $s_1 = s_2 = -1$, substituting Eq. (6) into Eq. (3) yields

$$-\partial_\tau^2\phi_1 - \phi_1 + \left[\phi_2(0) + \frac{\tau^2}{2}\phi_2''(0)\right]\phi_1 = 0. \tag{7}$$

Equation (7) is the SMM [28]. Based on the SMM we can get the analytical soliton solutions symmetric about $x = 0$, which are taken as the initial trial solutions to get the numerical solutions. The numerical solutions of the asymmetric solitons can also be gotten by tailoring the symmetric ones as the trial solutions.

It is well-known that the SMM has the analytical solution in the following form [28]:

$$\phi_1(\tau) = \frac{\sqrt{P_0}}{(w_0\sqrt{\pi})^{1/2}}\exp\left(-\frac{\tau^2}{2w_0^2}\right), \tag{8}$$

where P_0 is the input power of ϕ_1 and w_0 is the beam width of the pulse duration. Substituting Eq. (8) into Eq. (7) yields

$$\phi_2(0) = 1 - \frac{1}{w_0^2}, \tag{9}$$

$$\phi_2''(0) = \frac{2}{w_0^4}. \tag{10}$$

Therefore, if the relation between the input power of ϕ_1 (i.e., P_0) and $\phi_2(0)$ as well as $\phi_2''(0)$ is known, one can get the power P_0 and the beam width w_0 in the solution Eq. (8). In the following the relation is established by solving Eq. (4).

To investigate the bright nonlocal quadratic solitons induced by boundary confinement, We take into account the setup composed of the parametric material and air (Fig. 1). For the TE-polarized waves, the boundary conditions are [29]

$$\phi_{1,2}(-L/2 + 0) = \phi_{1,2}(-L/2 - 0), \tag{11}$$

$$\partial_\tau\phi_{1,2}(-L/2 + 0) = \partial_\tau\phi_{1,2}(-L/2 - 0), \tag{12}$$

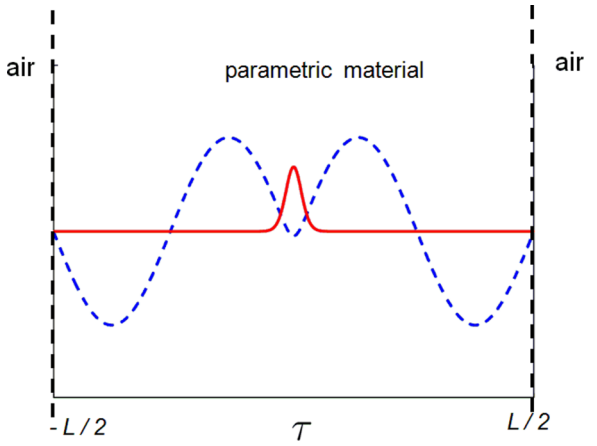

FIG. 1. Sketch of the bright nonlocal quadratic soliton induced by boundary confinement in the setup composed of parametric material and air. Red solid and blue dashed lines represent the FW and the SH, respectively.

$$\phi_{1,2}(L/2+0) = \phi_{1,2}(L/2-0), \tag{13}$$

$$\partial_\tau \phi_{1,2}(L/2+0) = \partial_\tau \phi_{1,2}(L/2-0). \tag{14}$$

For the TM-polarized waves, the boundary conditions for the transverse magnetic field can be expressed in a similar fashion. Hence, the TM-polarized surface waves can be dealt with in a similar way. Alfassi *et al.* [29] have shown the fact that, if the index difference between the two materials on two sides of the interface is significant, the optical energy is almost totally confined in the nonlocal nonlinear medium, whether the wave is TE or TM polarized. Therefore, for the setup composed of the parametric material and air, we can approximately regard the boundary conditions as the Dirichlet boundary conditions:

$$\phi_1(-L/2) = \phi_1(+L/2) = 0, \quad \phi_2(-L/2) = \phi_2(+L/2) = 0, \tag{15}$$

For the FWs' ϕ_1, so long as $w_0 \ll L$, the trial solution Eq. (8) will naturally satisfy the boundary conditions; and the boundary has little direct influence on the FWs. Whereas for the SHs' ϕ_2, which are oscillatory, they will be crucially influenced by the boundary.

For Eq. (4) which governs ϕ_2, the solution ϕ_2 is the sum of the general solution $[\phi_2^{(1)}(\tau)]$ of the homogeneous equation and the particular solution $[\phi_2^{(2)}(\tau)]$ of the inhomogeneous equation, i.e.,

$$\phi_2(\tau) = \phi_2^{(1)}(\tau) + \phi_2^{(2)}(\tau). \tag{16}$$

Providing the soliton is symmetric about the center of the sample, the general solution should be

$$\phi_2^{(1)}(\tau) = c_1 \cos(\sqrt{\alpha}\tau) \tag{17}$$

according to the symmetry characteristic. The particular solution of the inhomogeneous Eq. (4) is

$$\phi_2^{(2)}(\tau) = \frac{1}{4\sqrt{\alpha}} \int_{-\infty}^{\infty} \phi_1^2(\xi) \sin(\sqrt{\alpha}|\tau - \xi|) d\xi. \tag{18}$$

In order to get the parameter c_1, the boundary conditions and the particular solution at the boundary should be taken into account. Now let's substitute the soliton solution [Eq. (8)] into Eq. (18) to get the particular solution at the boundary. Because the field ϕ_1 has intensity only in the region $-L/2 < \xi < L/2$, we can make the approximation

$$\begin{aligned}\phi_2^{(2)}\left(\frac{L}{2}\right) &\approx \frac{1}{4\sqrt{\alpha}} \int_{-\infty}^{\infty} \left[\frac{\sqrt{P_0}}{(w_0\sqrt{\pi})^{1/2}} \exp\left(-\frac{\tau^2}{2w_0^2}\right)\right]^2 \\ &\quad \times \sin[\sqrt{\alpha}(\tau - \xi)] d\xi \\ &= \frac{P_0}{4\sqrt{\alpha}} \exp\left(-\frac{\alpha}{4} w_0^2\right) \sin\left(\frac{\sqrt{\alpha}}{2} L\right).\end{aligned} \tag{19}$$

In a similar way

$$\phi_2^{(2)}\left(-\frac{L}{2}\right) \approx \frac{P_0}{4\sqrt{\alpha}} \exp\left(-\frac{\alpha}{4} w_0^2\right) \sin\left(\frac{\sqrt{\alpha}}{2} L\right). \tag{20}$$

At the boundary, the particular solution $\phi_2^{(1)}(\pm L/2)$ and the general solution $\phi_2^{(2)}(\pm L/2)$ together satisfy the boundary condition Eq. (15), i.e.,

$$\phi_2^{(1)}\left(\pm\frac{L}{2}\right) + \phi_2^{(2)}\left(\pm\frac{L}{2}\right) = 0. \tag{21}$$

Therefore we get

$$c_1 = -\frac{P_0}{4\sqrt{\alpha}} \exp\left(-\frac{\alpha}{4} w_0^2\right) \tan\left(\frac{\sqrt{\alpha}}{2} L\right), \tag{22}$$

and then

$$\begin{aligned}\phi_2(\tau) = &\frac{1}{4\sqrt{\alpha}} \int_{-\infty}^{\infty} \phi_1^2(\xi) \sin\left(\sqrt{\alpha}|\tau - \xi|\right) d\xi \\ &- \frac{P_0}{4\sqrt{\alpha}} \exp\left(-\frac{\alpha}{4} w_0^2\right) \tan\left(\frac{\sqrt{\alpha}}{2} L\right) \cos(\sqrt{\alpha}\tau).\end{aligned} \tag{23}$$

Making a Taylor expansion to Eq. (23) with respect to τ to the second order yields

$$\phi_2(\tau) \approx \phi_2(0) + \frac{\tau^2}{2} \phi_2''(0), \tag{24}$$

where

$$\begin{aligned}\phi_2(0) = &\frac{P_0}{2\sqrt{\pi\alpha}} F_{\mathrm{ds}}\left(\frac{\sqrt{\alpha}}{2} w_0\right) \\ &- \frac{P_0}{4\sqrt{\alpha}} \exp\left(-\frac{\alpha}{4} w_0^2\right) \tan\left(\frac{L\pi}{T_s}\right),\end{aligned} \tag{25}$$

$$\phi_2''(0) = \frac{P_0}{2\sqrt{\pi} w_0} - \alpha \phi_2(0). \tag{26}$$

F_{ds} represents the Dawson integral, and $T_s = 2\pi/\sqrt{\alpha}$ is the oscillatory period of the SHs.

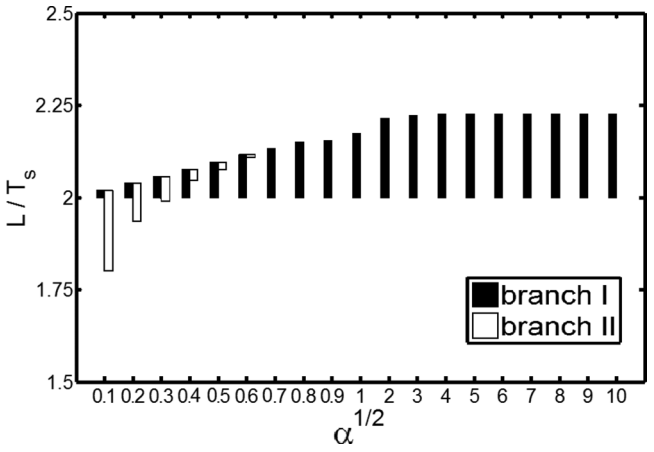

FIG. 2. The existence domain for the two branches of symmetric single-hump bright solitons in one period (the sample size varies from $1.5T_s$ to $2.5T_s$) for various degree of nonlocality (the nonlocal degree becomes weaker with the increase of $\sqrt{\alpha}$).

Comparing Eqs. (9) and (10) with Eqs. (25) and (26), we get

$$P_0 = 2\sqrt{\pi}w_0\left[\alpha\left(1-\frac{1}{w_0^2}\right)+\frac{2}{w_0^4}\right], \tag{27}$$

$$P_0 = 4\sqrt{\pi\alpha}\left(1-\frac{1}{w_0^2}\right)\left[2F_{\rm ds}\left(\frac{\sqrt{\alpha}}{2}w_0\right) - \sqrt{\pi}\exp\left(-\frac{\alpha}{4}w_0^2\right)\tan\left(\frac{L\pi}{T_s}\right)\right]^{-1}, \tag{28}$$

which yield

$$2F_{\rm ds}\left(\frac{\sqrt{\alpha}}{2}w_0\right) - \sqrt{\pi}\exp\left(-\frac{\alpha}{4}w_0^2\right)\tan\left(\frac{L\pi}{T_s}\right) = \frac{\frac{2\sqrt{\alpha}}{w_0}\left(1-\frac{1}{w_0^2}\right)}{\alpha\left(1-\frac{1}{w_0^2}\right)+\frac{2}{w_0^4}}. \tag{29}$$

Based on Eq. (29) one can get the soliton width w_0, and in turn get the power P_0 based on Eq. (27) or (28), and the corresponding SHs can be obtained from Eq. (23). If the solution satisfies the prerequisite that $0 < w_0 < T_s/2$ and $P_0 > 0$, we regard it as a reasonable soliton solution, to which the SMM is applicable. In the following we take the Gaussian solution [i.e., Eq. (8)] with the reasonable w_0 and P_0 as the initial trial solution to find the numerical solutions of Eqs. (3) and (4) based on the Newton iteration approach.

III. NUMERICAL RESULT

Equations (27)–(29) may have none, one, two, or several center-symmetric solutions for different sample sizes L and nonlocal degrees α. We take the physically reasonable and

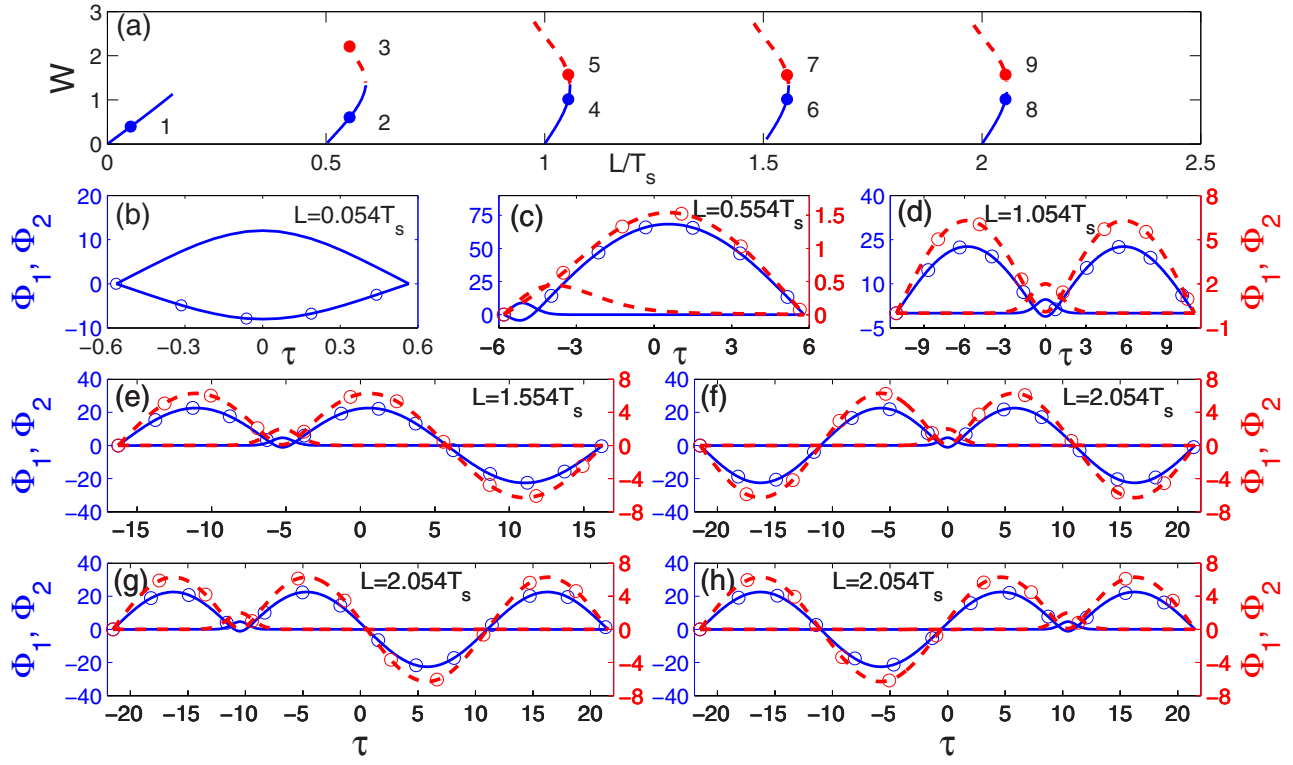

FIG. 3. (a) The rms width w for ϕ_1 of branch I (blue solid lines) and branch II (red dashed lines) solitons versus sample size L, when $\sqrt{\alpha} = 0.3$. (b)–(h) Soliton profiles of branch I [blue solid lines (FW) and blue solid lines with circle symbol (SH), left ordinate] and branch II [red dashed lines (FW) and red dashed lines with circle symbol (SH), right ordinate] for different sample sizes corresponding to points 1–9 in panel (a). Panels (f)–(h) all correspond to points 8 and 9, but the FWs are located at different positions of the sample.

SMM-applicable solutions (which satisfy the prerequisite that $0 < w_0 < T_s/2$ and $P_0 > 0$) as trial solutions to find the numerical solutions based on the Newton iteration approach. According to the numerical results we get two branches of solitons shown in Figs. 2 and 3. In general, the forms of FWs are bell-like, and those of the SHs are oscillatory.

After getting the central-symmetric solitons, we guess that, according to the oscillatory form of the SHs, one may get new center-asymmetric solitons if the central-symmetric solitons are properly shifted. Based on this guess, we shift and tailor the central-symmetric solution as the initial guess. Through the Newton iteration approach we get the numerical solution which is in accordance with our guess [as shown in Figs. 3(c), 3(e), 3(g), and 3(h)].

Figure 2 shows the distribution of the bright solitons in one period (the sample size varies from $1.5T_s$ to $2.5T_s$) for various degrees of nonlocality. It shows that there exist two branches of solitons, of which the beam width increases and decreases with the increase of the sample size, respectively [Fig. 3(a)].

Branch I solitons (the beam width increases with the sample size, represented with blue bars in Fig. 3) exist for all the degrees of nonlocality we investigated. The lower limit for the existence regime of the branch I soliton is fixed at $L = 2T_s$ for every degree of nonlocality, but the upper limit varies with the degree of nonlocality. Specifically speaking, the existence regime is relatively narrow for strong nonlocality (corresponding tothe small value of $\sqrt{\alpha}$), then increases with the decrease of nonlocality (i.e., the increase of $\sqrt{\alpha}$), and at last keeps invariant for the relatively weak nonlocality ($\sqrt{\alpha} > 2$).

However, the branch II solitons (the beam width decreases with the sample size, represented with red bars in Fig. 3) exist only in the relatively stronger nonlocal case ($\sqrt{\alpha} < 0.6$), and the stronger the nonlocality is, the wider the existence regime will be. Unlike the branch I solitons, both the lower limit and the upper limit for the existence regime of the branch II solitons increase with the decrease of nonlocality (i.e., the increase of $\sqrt{\alpha}$). In addition, the upper limit of branch I is very close to that of branch II, if both two branches for the considered degree of nonlocality exist.

If the nonlocality is fixed and the sample size is varied, the soliton width varies piecewise and approximately periodically [the period is $T_s/2$, Fig. 3(a)]. In every period, there is only a small range of sample sizes in which solitons exist. The width of the Branch I (II) solitons increases (decreases) with the increase of the sample size in each period. There are some major characteristics of the two branches of solitons.

(1) The solitons can be (but not necessarily) symmetric about the sample center in the range $mT_s < L < (m + 1/2)T_s$ ($m = 0,1,2,\ldots$), but are undoubtedly asymmetric about the sample center in the range $(m + 1/2)T_s < L < (m + 1)T_s$.

(2) In the first interval ($0 < L < T_s/2$) only the branch I solitons exist; the branch II solitons do not exist [Fig. 3(b)]. In the second and following intervals ($L > T_s/2$) both branch I and branch II solitons exist.

(3) Under the Dirichlet boundary conditions, the soliton is formed if (i) the diffraction of the FW soliton is balanced by the nonlinear effect or (ii) the boundary effect together with the nonlinear effect balances the diffraction. In the first case, the distribution of the FW is a bell-like one [Figs. 3(c)–3(g)]. But in the second case, the distribution of the FW approximate to the boundary deviates from the bell-like form [Figs. 3(a) and 3(b)].

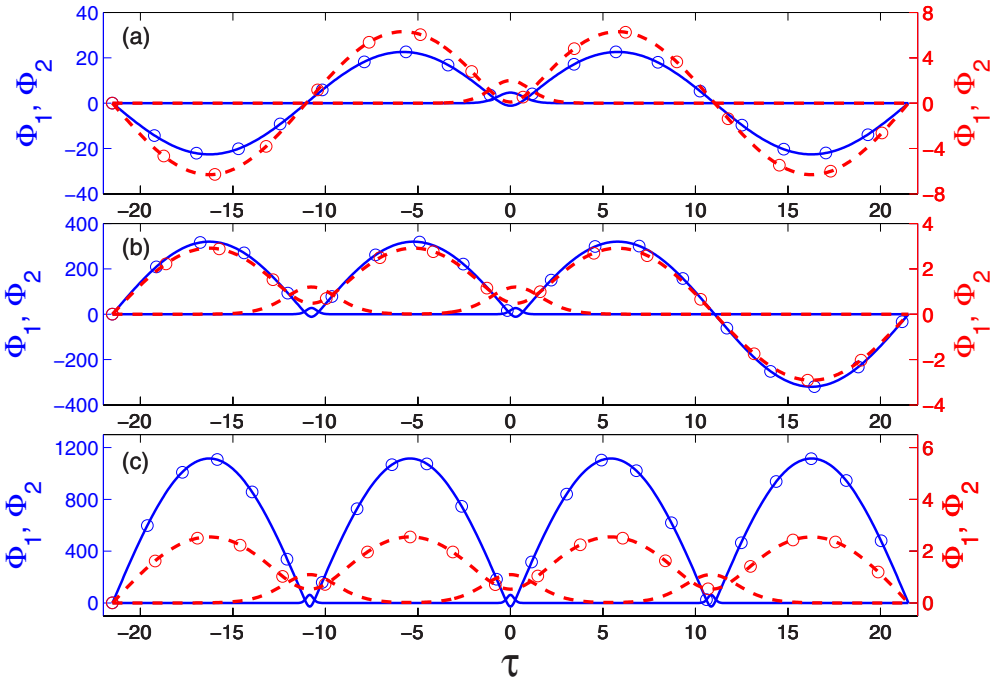

FIG. 4. (a) The single-hump branch I [blue solid lines (FW) and blue solid lines with circle symbol (SH), left ordinate] and branch II [red dashed lines (FW) and red dashed lines with circle symbol (SH), right ordinate] solitons in the sample for $L = 2.054T_s$ and $\sqrt{\alpha} = 0.3$. (b) The double-hump solitons in the sample with the same parameters. (c) The triple-hump solitons in the sample with the same parameters.

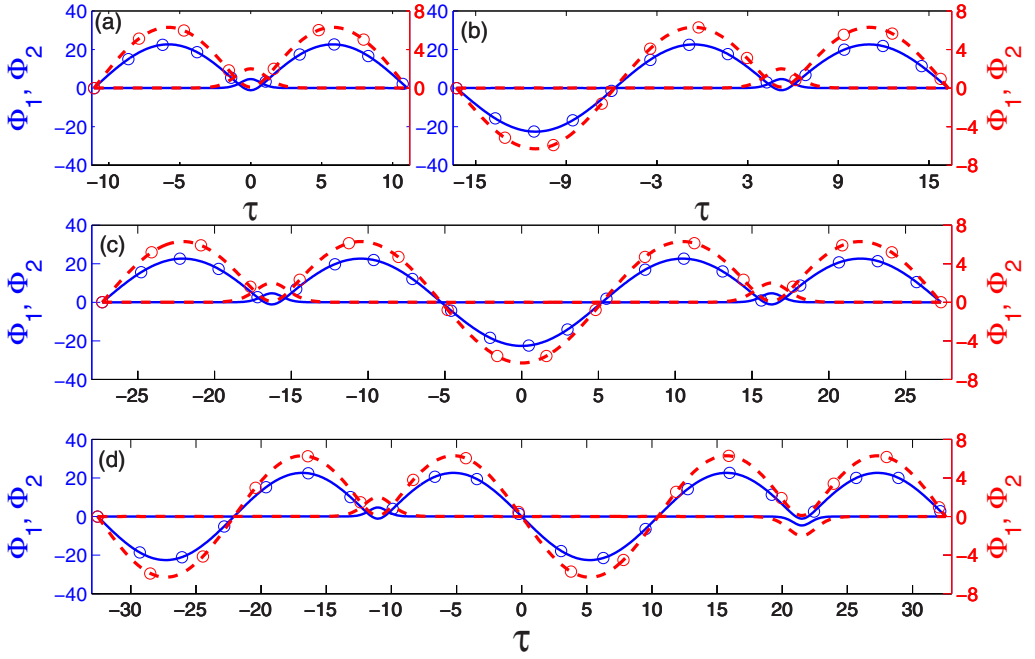

FIG. 5. (a) The single-hump branch I [blue solid lines (FW) and blue solid lines with circle symbol (SH), left ordinate] and branch II [red dashed lines (FW) and red dashed lines with circle symbol (SH), right ordinate] solitons in the sample with the size $L_1 = 1.05T_s$. (b) The single-hump branch I and branch II solitons in the sample with the size $L_2 = 1.554T_s$. (c) The double-hump branch I and branch II solitons in the sample with the size $L = L_1 + L_2$. (d) The double-hump branch I and branch II solitons in the sample with the size $L = 2L_2$. In panels (a)–(d) $\sqrt{\alpha} = 0.3$.

(4) For a fixed sample size, the FW soliton can be located at different positions of the sample, providing the left- and right-hand sides have integral numbers of half-sine oscillation [Figs. 3(f)–3(h)].

(5) In the third and following intervals, if there exist solitons (not approximate to the boundary) in two samples with size $L = l_1$ and $L = l_2 = l_1 + mT_s/2$, the soliton in the sample with $L = l_2$ is the extension of that in the sample with $L = l_1$. In other words, the shape and the size of the two FWs approximate very well to each other, and the SH of the sample with $L = l_2$ has m more half-oscillatory periods than that of the sample with $L = l_1$.

Figure 4 shows that in a sample with a fixed degree of nonlocality ($\sqrt{\alpha} = 0.3$) and a fixed sample size ($L = 2.054T_s$), there may exist single- and multihump solitons. The more the number of humps for the branch I (branch II) solitons is, the narrower (wider) the width will be.

As shown in Fig. 5, if in samples with sizes $L_1 = m_1T_s/2 + l$, $L_2 = m_2T_s/2 + l, \ldots$, and $L_p = m_pT_s/2 + l$ exist single-hump solitons with the same width, in the sample with size $L = L_1 + L_2 + \cdots + L_p$ will exist a p-hump soliton (the hump can be in-phase or out-of-phase), which looks to be jointed by the single-hump solitons, as long as the SHs for the single-hump solitons are connected smoothly. It should be noted that, only the same branch solitons can be "jointed"; the branch I soliton(s) cannot be "jointed" with the branch II solitons, because the two types of solitons have obviously different widths and amplitudes, as shown in Fig. 3.

We have propagated the two branches of solitons with various parameters to study their stability. In simulating the propagation of the found solitons, Eqs. (1) and (2) are used; the Dirichlet boundary conditions, i.e., $E_1(-L/2) = E_1(+L/2) = 0$, $E_2(-L/2) = E_2(+L/2) = 0$, are addressed;

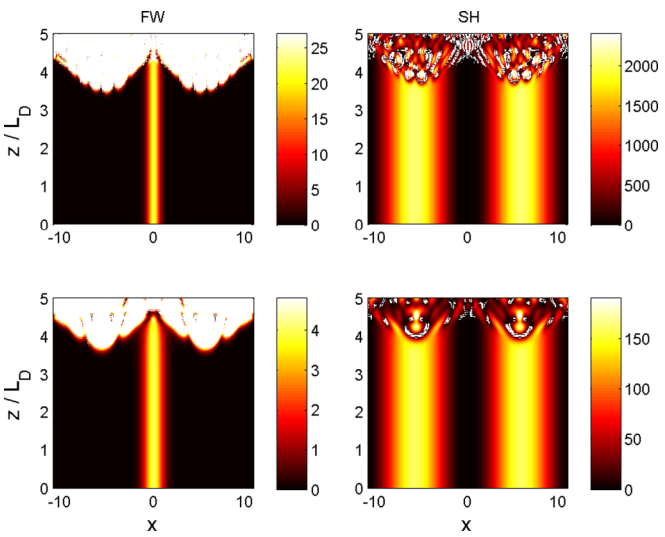

FIG. 6. Upper panels: Intensity evolution of FW (left) and SH (right) of the branch I soliton for $L = 1.054T_s$ and $\sqrt{\alpha} = 0.3$. Lower panels: Evolution of FW (left) and SH (right) for the branch II soliton; the parameters are the same as those for the upper panels. The simulation used $d_1 = 2$, $d_2 = 1$, $\lambda = -2$, and $N_x = 339$ (for branch I) and $N_x = 259$ (for branch II) points in x and $N_z = 5 \times 10^4$ steps in z (corresponding to that the step length along z is $\Delta z = L_d/10^4$, where $L_D = w^2/(2|d_1|)$ is the Rayleigh distance of the FW and w is the rms width of the FW.)

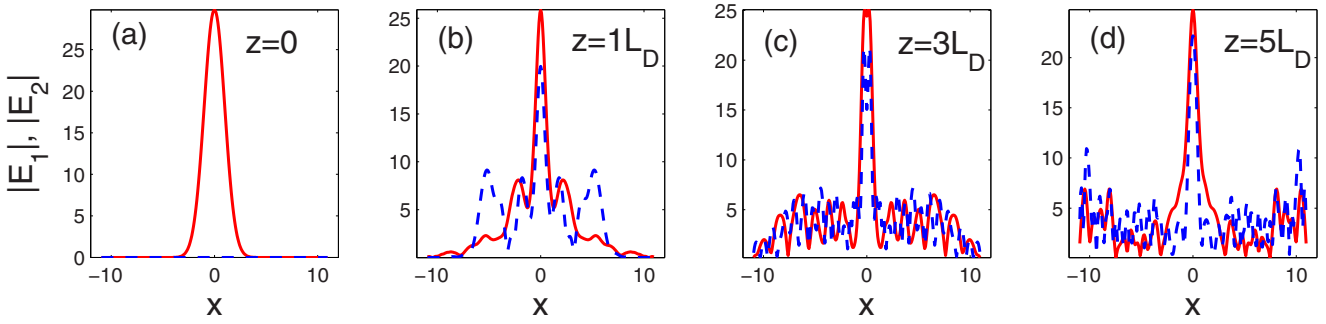

FIG. 7. An example for the evolution of FW (red solid line) and SH (blue dashed line) for the case that only the FW beam (with Gaussian profile) is input. At the entrance plane the width of the FW equals that of the FW of the branch II soliton for $L = 1.054T_s$ and $\sqrt{\alpha} = 0.3$, and the power equals the total power of the FW and the SH of the branch II soliton. Other parameters are the same as those in Fig. 6.

and a code with a finite difference method is used. We have checked a conserved quantity, i.e., the total power. It is conserved during propagation. The result shows that the two branches of solitons are all unstable. As shown in Fig. 6 for example, the solitons can only keep the shape in a few Rayleigh distances L_D of the FW [defined as $L_D = w^2/(2|d_1|)$, w is the rms width of the FW] and then break up quickly (Fig. 6).

For the case $s_{1,2=-1}$, it is the Dirichlet boundary conditions which makes the relation between the FWs and the SHs of the solitons differ from that under the no-boundary conditions; and it causes the existence of bright solitons (which is not found under the no-boundary conditions). In the view of geometrical optics, the beam undergoes total internal reflection at the interface between the quadratic material and the air during propagation, this might be the reason for the instability of the found two branches of solitons.

We have also simulated the propagation of Gaussian beams in the sample for different sample sizes and beam powers (e.g., Fig. 7). The result shows that the power interchange between the FW and the SH happens when the FW diffracts during propagation. The power interchange and the diffraction interact; this make the beam shape change greatly. After the arrival of the beam edge at the boundary, the shape changes more dramatically. Because of the combined action of diffraction, power interchange, and boundary confinement, the Gaussian beams undergo complicated propagation; we have not found a general law for their propagation. In fact, the irregular propagation of Gaussian beams is as expected: even for the soliton solutions, the beam is unstable and quickly breaks up during propagation. For the Gaussian beams which are greatly different from the soliton solutions (with bell-like FW as well as oscillating SH), the propagation would be much more unstable and irregular.

IV. CONCLUSION

In conclusion, under the Dirichlet boundary conditions there can exist bright parametric solitons in the case $s_1 = s_2 = -1$, in which only dark solitons are found under the no-boundary conditions in previous works. If the model Eqs. (3) and (4) are reduced into the SMM model, one can get the approximate analytical solution of the bright solitons, which can be taken as the initial trial function to get the numerical precise solution. The numerical results show that the bright solitons in the case $s_1 = s_2 = -1$ can be classified into two branches, i.e., branch I and branch II, of which the beam width increases and decreases with the increase of the sample size, respectively. Branch I solitons exist in all the degrees of nonlocality we investigated; but the branch II solitons exist only in the stronger nonlocal case. If the nonlocality is fixed and the sample size is varied, the soliton width varies piecewise and approximately periodically. In every period, there is only a small range of sample sizes in which soliton exists. In a sample with fixed degree of nonlocality and fixed sample size, there may exist single- and multihump solitons. The more the number of humps for the branch I (branch II) solitons is, the narrower (wider) the width will be. In addition, single-hump solitons with the same beam width of FWs in narrower samples can be jointed to be a multihump soliton in a wider sample (the size is the sum of those of the narrower ones), as long as the SHs for the single-hump FW solitons are connected smoothly. Our results only cover the solitons of which the SMM is applicable and the forms of the FWs and SHs are bell-like and oscillatory, respectively. There may be other soliton solutions differing from our result or beyond the SMM, but they call for other initial guesses, theoretical modes, and further exploration.

ACKNOWLEDGMENT

This research was supported by the National Natural Science Foundation of China (Grants No. 11174090, No. 11174091, and No. 61575068).

[1] Y. N. Karamzin and A. P. Sukhorukov, Nonlinear interaction of diffracted light beams in a medium with quadratic nonlinearity: Mutual focusing of beams and limitation on the efficiency of optical frequency converters, JETP Lett. **20**, 339 (1974).

[2] Y. N. Karamzin and A. P. Sukhorukov, Mutual focusing of high-power light beams in media with quadratic nonlinearity, Sov. Phys. JETP **41**, 414 (1976).

[3] W. E. Torruellas, Z. Wang, D. J. Hagan, E. W. VanStryland, G. I. Stegeman, L. Torner, and C. R. Menyuk, Observation of Two-

Dimensional Spatial Solitary Waves in a Quadratic Medium, Phys. Rev. Lett. **74**, 5036 (1995).

[4] R. Schiek, Y. Baek, and G. I. Stegeman, One-dimensional spatial solitary waves due to cascaded second-order nonlinearities in planar waveguides, Phys. Rev. E **53**, 1138 (1996).

[5] A. V. Buryak, P. D. Trapani, D. V. Skryabin, and S. Trillo, Optical solitons due to quadratic nonlinearities: From basic physics to futuristic applications, Phys. Rep. **370**, 63 (2002).

[6] L. Torner and A. Barthélémy, Quadratic solitons: Recent developments, IEEE J. Quantum Electron. **39**, 22 (2003).

[7] Yu. S. Kivshar and G. P. Agrawal, *Optical Solitons: From Fibers to Photonic Crystals* (Academic, San Diego, 2003).

[8] G. Assanto and G. I. Stegeman, Simple physics of quadratic spatial solitons, Opt. Express **10**, 388 (2002).

[9] W. E. Torruellas, G. Assanto, B. L. Lawrence, R. A. Fuerst, and G. I. Stegeman, All-optical switching by spatial walkoff compensation and solitary-wave locking, Appl. Phys. Lett. **68**, 1449 (1996).

[10] C. B. Clausen, O. Bang, and Y. S. Kivshar, Spatial Solitons and Induced Kerr Effects in Quasi-Phase-Matched Quadratic Media, Phys. Rev. Lett. **78**, 4749 (1997).

[11] J. F. Corney, and O. Bang, Solitons in quadratic nonlinear photonic crystals, Phys. Rev. E **64**, 047601 (2001).

[12] J. F. Corney, and O. Bang, Modulational Instability in Periodic Quadratic Nonlinear Materials, Phys. Rev. Lett. **87**, 133901 (2001).

[13] A. Kobyakov, A. Kobyakov, F. Lederer, O. Bang, and Y. S. Kivshar, Nonlinear phase shift and all-optical switching in quasi-phase-matched quadratic media, Opt. Lett. **23**, 506 (1998).

[14] O. Bang, T. W. Graversen, and J. F. Corney, Accurate switching intensities and length scales in quasi-phase-matched materials, Opt. Lett. **26**, 1007 (2001).

[15] O. Bang, Dynamical equations for wave packets in materials with both quadratic and cubic response, J. Opt. Soc. Am. B **14**, 51 (1997).

[16] C. R. Menyuk, R. Schiek, and L. Tornert, Solitary waves due to $\chi^{(2)}:\chi^{(2)}$ cascading, J. Opt. Soc. Am. B **11**, 2434 (1994).

[17] N. I. Nikolov, D. Neshev, O. Bang, and W. Z. Królikowski, Quadratic solitons as nonlocal solitons, Phys. Rev. E **68**, 036614 (2003).

[18] G. I. Stegeman, D. J. Hagan, and L. Torner, Cascading phenomena and their applications to all-optical signal processing, mode-locking, pulse compression and solitons, Opt. Quantum Electron. **28**, 1691 (1996).

[19] W. Królikowski, O. Bang, N. I. Nikolov, D. Neshev, J. Wyller, J. J. Rasmussen, and D. Edmundson, Modulational instability, solitons and beam propagation in nonlocal nonlinear media, J. Opt. B **6**, S288 (2004).

[20] M. Bache, O. Bang, J. Moses, and F. W. Wise, Nonlocal explanation of stationary and nonstationary regimes in cascaded soliton pulse compression, Opt. Lett. **32**, 2490 (2007).

[21] M. Bache, O. Bang, W. Królikowski, J. Moses, and F. W. Wise, Limits to compression with cascaded quadratic soliton compressors, Opt. Express **16**, 3273 (2008).

[22] P. V. Larsen, M. P. Sorensen, O. Bang, W. Z. Królikowski, and S. Trillo, Nonlocal description of X waves in quadratic nonlinear materials, Phys. Rev. E **73**, 036614 (2006).

[23] J. Wyller, W. Królikowski, O. Bang, D. E. Petersen, and J. J. Rasmussen, Modulational instability in the nonlocal $\chi^{(2)}$-model, Phys. D **227**, 8 (2007).

[24] C. Conti, M. A. Schmidt, P. S. J. Russell, and F. Biancalana, Highly Noninstantaneous Solitons in Liquid-Core Photonic Crystal Fibers, Phys. Rev. Lett. **105**, 263902 (2010).

[25] A. V. Buryak and Y. S. Kivshar, Solitons due to second harmonic generation, Phys. Lett. A **197**, 407 (1995).

[26] B. K. Esbensen, M. Bache, W. Królikowski, and O. Bang, Quadratic solitons for negative effective second-harmonic diffraction as nonlocal solitons with periodic nonlocal response function, Phys. Rev. A **86**, 023849 (2012).

[27] J. Wang, Y. Li, Q. Guo, and W. Hu, Stabilization of nonlocal solitons by boundary conditions, Opt. Lett. **39**, 405 (2014).

[28] A. W. Snyder and D. J. Mitchell, Accessible solitons, Science **276**, 1538 (1997).

[29] B. Alfassi, C. Rotschild, O. Manela, M. Segev, and D. N. Christodoulides, Nonlocal Surface-Wave Solitons, Phys. Rev. Lett. **98**, 213901 (2007).